POLYMER CHEMISTRY

Visible light–triggered depolymerization of commercial polymethacrylates

Hyun Suk Wang[1], Mikhail Agrachev[2], Hongsik Kim[3], Nghia P. Truong[1], Tae-Lim Choi[3], Gunnar Jeschke[2], Athina Anastasaki[1]*

The reversion of vinyl polymers with carbon-carbon backbones to their monomers represents an ideal path to alleviate the growing plastic waste stream. However, depolymerizing such stable materials remains a challenge, with state-of-the-art methods relying on "designer" polymers that are neither commercially produced nor suitable for real-world applications. In this work, we report a main chain–initiated, visible light–triggered depolymerization directly applicable to commercial polymers containing undisclosed impurities (e.g., comonomers, additives, or dyes). By in situ generation of chlorine radicals directly from the solvent, near-quantitative (>98%) depolymerization of polymethacrylates could be achieved regardless of their synthetic route (e.g., radical or ionic polymerization), end group, and molecular weight (up to 1.6 million daltons). The possibility to perform multigram-scale depolymerizations and confer temporal control renders this methodology a versatile and general route to recycling.

Although indispensable in our daily lives, plastics have led to serious environmental concerns ranging from landfill accumulation to microplastic contamination. Addressing these challenges necessitates a transition to a circular economy through recycling. Unfortunately, the predominant method, thermomechanical recycling, results in downcycling into lower-grade products through reduction of molecular weight (*1*, *2*). To circumvent product deterioration, alternatives such as "(photochemical) upcycling" (*3*–*10*) and chemical recycling to monomer (*1*, *11*, *12*) have been explored. Chemical recycling is a highly appealing option, as it not only establishes the smallest closed-loop cycle but also circumvents product deterioration (i.e., downcycling) through the synthesis of virgin-grade materials, with the option of even upgrading their properties (*1*, *13*). Vinyl polymers possess all-carbon backbones that render them chemically stable (e.g., from hydrolysis) but challenging to deconstruct owing to the absence of any heteroatom-associated weak links. The most conventional approach to break these bonds is pyrolysis, an industrially important reaction, but the extreme temperatures required (>400°C) lead to energy waste and undesirable byproducts. For example, pyrolysis of poly(methyl methacrylate) (PMMA) leads to formation of 2,3-butanedione, a compound that imparts a pungent odor to the recycled PMMA (*14*).

To alleviate these hurdles, polymers with preinstalled labile groups have recently been explored, the vast majority of which are synthesized by reversible deactivation radical polymerization (RDRP), also known as controlled radical polymerization (*15*–*20*). RDRP enables the production of well-defined polymers and precise control over their macromolecular characteristics, including architecture, sequence, dispersity, molecular weight, and end-group fidelity. Labile chain ends, usually halogens or thiocarbonylthio compounds, not only allow for the controlled synthesis of block copolymers but also facilitate depolymerization at lower temperatures than conventional pyrolysis (120° to 170°C) (*21*–*36*). The feasibility of depolymerizing RDRP polymers was first documented independently by the groups of Raus and Gramlich, who showed that low temperatures and high initial monomer concentrations are prerequisites for the successful polymerization of bulky monomers through atom transfer radical polymerization (ATRP) or reversible addition–fragmentation chain-transfer (RAFT) polymerization (*34*, *37*). Ouchi and co-workers then realized that the nonbulky PMMA could be partially depolymerized back to monomer, although low monomer recovery (i.e., up to 24%) was recorded and side reactions dominated the unzipping pathway (*35*). These seminal papers changed the perspective of the field, highlighted the possibility to trigger low-temperature depolymerizations, and initiated a number of exciting research directions. Matyjaszewski and co-workers demonstrated in a series of reports the full potential of halogen chain ends by using Cu or Fe halide salt catalysts to cleave the terminal C–Cl bond and achieve >80% depolymerization in solution and bulk (*23*–*25*). Sumerlin and co-workers used thiocarbonylthio esters to trigger depolymerization through photolytic cleavage of the terminal thiocarbonylthio C–S bond either in solution or a completely solvent-free process (*31*, *32*). More recently, the same group demonstrated depolymerization of PMMA triggered by thermolytically labile *N*-hydroxyphthalimide ester comonomers (*38*, *39*), whereas Diao and co-workers leveraged a comonomer-induced weak link in the backbone (*40*). Our group has also reported up to 92% depolymerization for various polymethacrylates using thiocarbonylthio– and halogen-terminated chain ends (*26*–*30*).

Despite these remarkable advances, these methods are restricted to "designer polymers" containing preinstalled weak links that render these materials thermally unstable. In fact, depolymerization of these materials relies precisely on their instability. Such polymers pose serious limitations for real-world applications and are not commercially produced. Thus, ATRP- or RAFT-based depolymerization strategies cannot

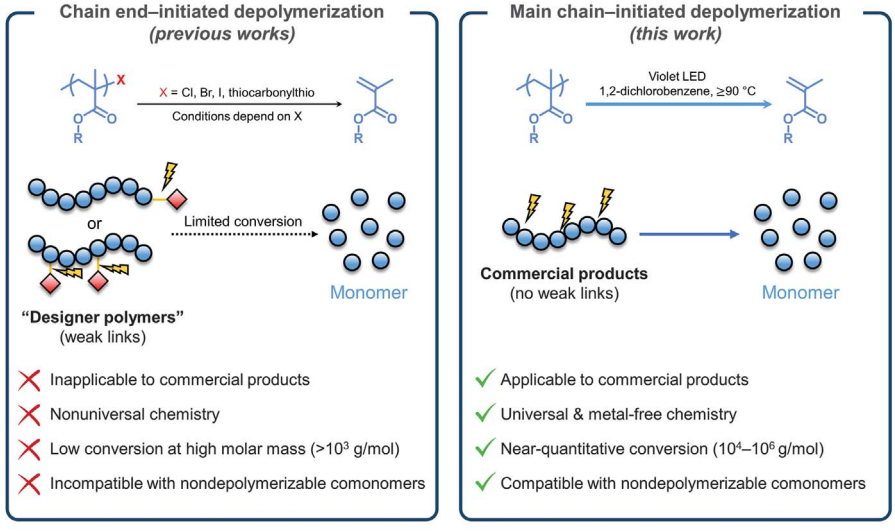

Fig. 1. Depolymerization approaches for PMMA. (Left) Chain end–initiated depolymerization through a labile chain end. (Right) Main chain–initiated depolymerization without the need for any labile group.

[1]Laboratory of Polymeric Materials, Department of Materials, ETH Zurich, Vladimir-Prelog-Weg 5, Zurich, Switzerland. [2]Institute for Molecular Physical Science, Department of Chemistry and Applied Biosciences, ETH Zurich, Vladimir-Prelog-Weg 2, Zurich, Switzerland. [3]Laboratory of Polymer Chemistry, Department of Materials, ETH Zurich, Vladimir-Prelog-Weg 5, Zurich, Switzerland.
*Corresponding author. Email: athina.anastasaki@mat.ethz.ch

address the annual inflow of 3.9 million metric tons of PMMA or existing waste (~90% unrecycled) (*41*, *42*). Notably, most end group–triggered depolymerizations are inherently limited to lower-molecular weight polymers and are severely affected by the presence of additional components (e.g., comonomers can prematurely quench depolymerization).

In this work, we report a one-step, near-quantitative, and visible light–triggered depolymerization of commercial PMMA that diverges from conventional methods through a main chain initiation pathway without reliance on any preinstalled weak bonds (Fig. 1). Notably, near-quantitative depolymerization can be achieved at high molecular weights (up to 10^6 g/mol) in the presence of nondepolymerizable comonomers and even after the polymer has been subjected to prolonged (solvo)thermal exposure. Our method is directly applicable to commercial products, such as Plexiglas, at a multigram scale (>10 g) without prior removal of the undisclosed additives contained within.

End group–independent depolymerization

A main chain–initiated depolymerization of vinyl polymers was serendipitously discovered while investigating the photothermal depolymerization of a high-molecular weight, dithiobenzoate-terminated PMMA (PMMA-DTB; number average molecular weight M_n = 212,500 g/mol, dispersity $Đ$ = 1.09) synthesized

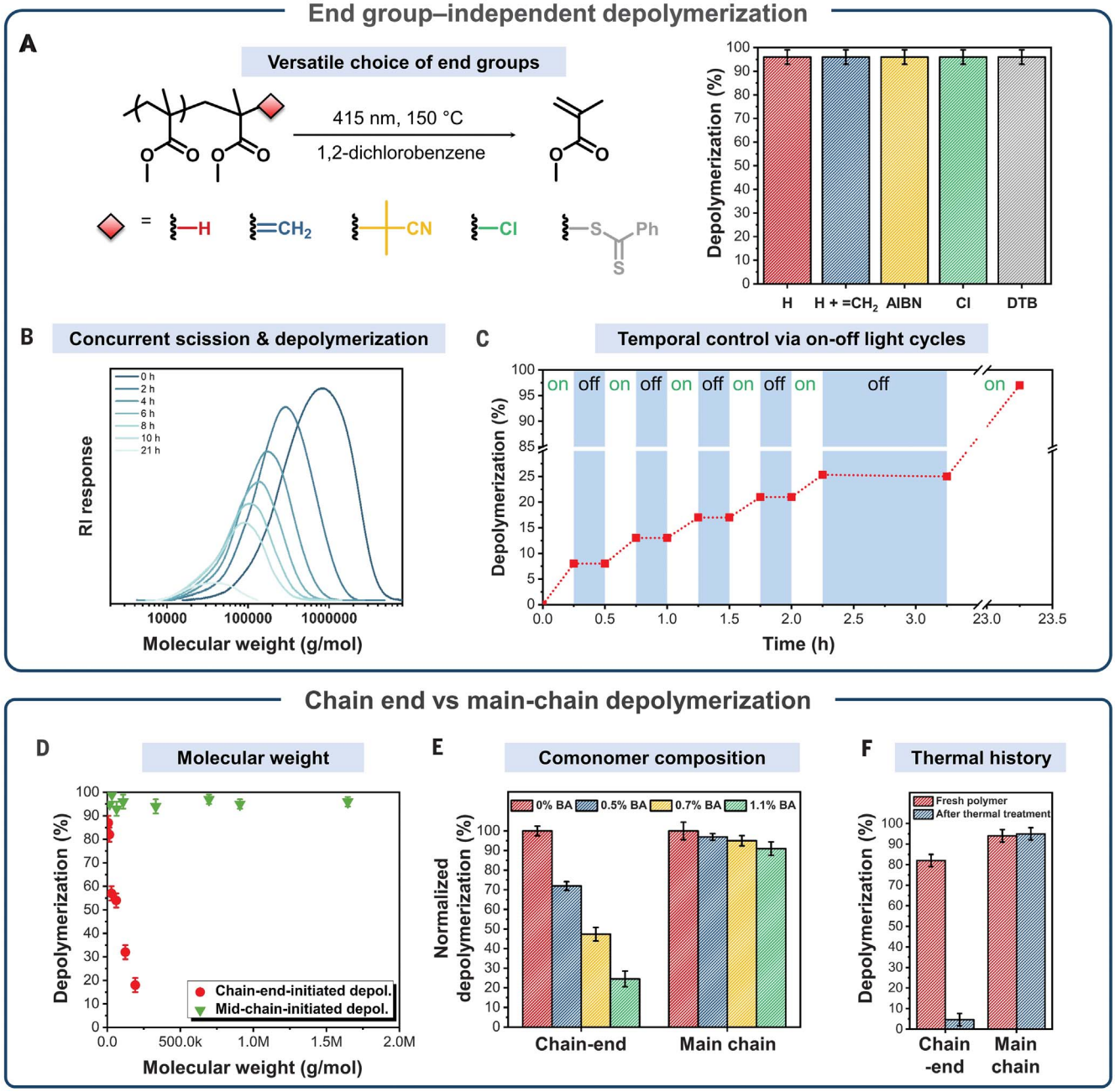

Fig. 2. Visible light–triggered depolymerization of PMMA through main chain initiation. (**A**) Depolymerization of PMMA with various end groups. AIBN, azobisisobutyronitrile. (**B**) SEC traces during depolymerization of PMMA synthesized by free radical polymerization. (**C**) Temporal control of depolymerization with on-off light cycles. Effect of (**D**) molecular weight, (**E**) BA content, and (**F**) thermal history on the final conversion for chain end– and main chain–initiated depolymerization. PMMA-DTB was used for chain end–initiated depolymerization. Error bars represent the standard deviation of >3 experiments.

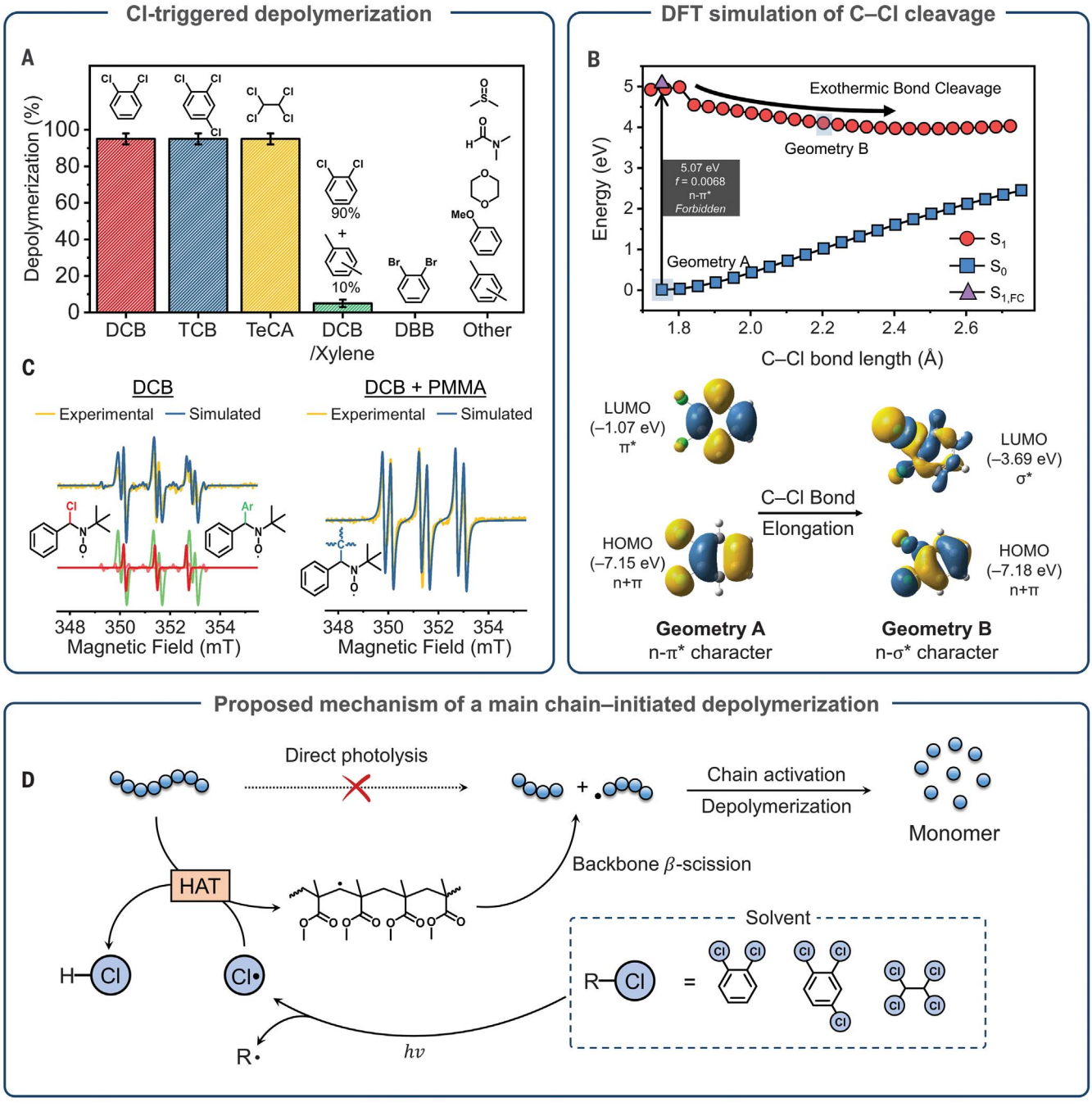

Fig. 3. Probing the mechanism of the main chain–initiated depolymerization. (**A**) Depolymerization conversions in different solvents under 415-nm irradiation. (**B**) DFT-calculated potential pathway for the photodissociation of DCB. *f*, oscillator strength; LUMO, lowest unoccupied molecular orbital; HOMO, highest occupied molecular orbital. (**C**) EPR spectra and simulations of irradiated DCB (left) and PMMA solution in DCB (right) in the presence of N-*tert*-butyl-α-phenylnitrone spin trap. (**D**) Proposed scheme of the HAT-induced depolymerization. Error bars represent the standard deviation of >3 experiments.

by RAFT polymerization (figs. S1 to S4). Depolymerization of PMMA-DTB in dioxane at 150°C and under ultraviolet (UV) irradiation led to no appreciable depolymerization after 6 hours (only ~10% conversion; fig. S3, A to D), in line with previous literature (*31*, *43*). Instead, when the reaction was repeated in 1,2-dichlorobenzene (DCB) under otherwise identical conditions, unusually high monomer recovery was observed (74%) within the same time frame (fig. S3F and table S1). Size exclusion chromatography (SEC) analysis of aliquots taken during the reaction in DCB showed an even greater decrease in molecular weight (90% reduction), indicating an unusual main chain scission depolymerization. Intrigued by these results, we screened various reaction conditions to further improve the conversion and discovered that near-quantitative depolymerization (>95%) of PMMA-DTB could be achieved at 150°C even under visible light (violet light–emitting diode, wavelength λ = 415 nm) irradiation (table S2).

We hypothesized that comparable depolymerization conversions could be reached regardless of the chain-end structure if indeed depolymerization proceeded through main chain

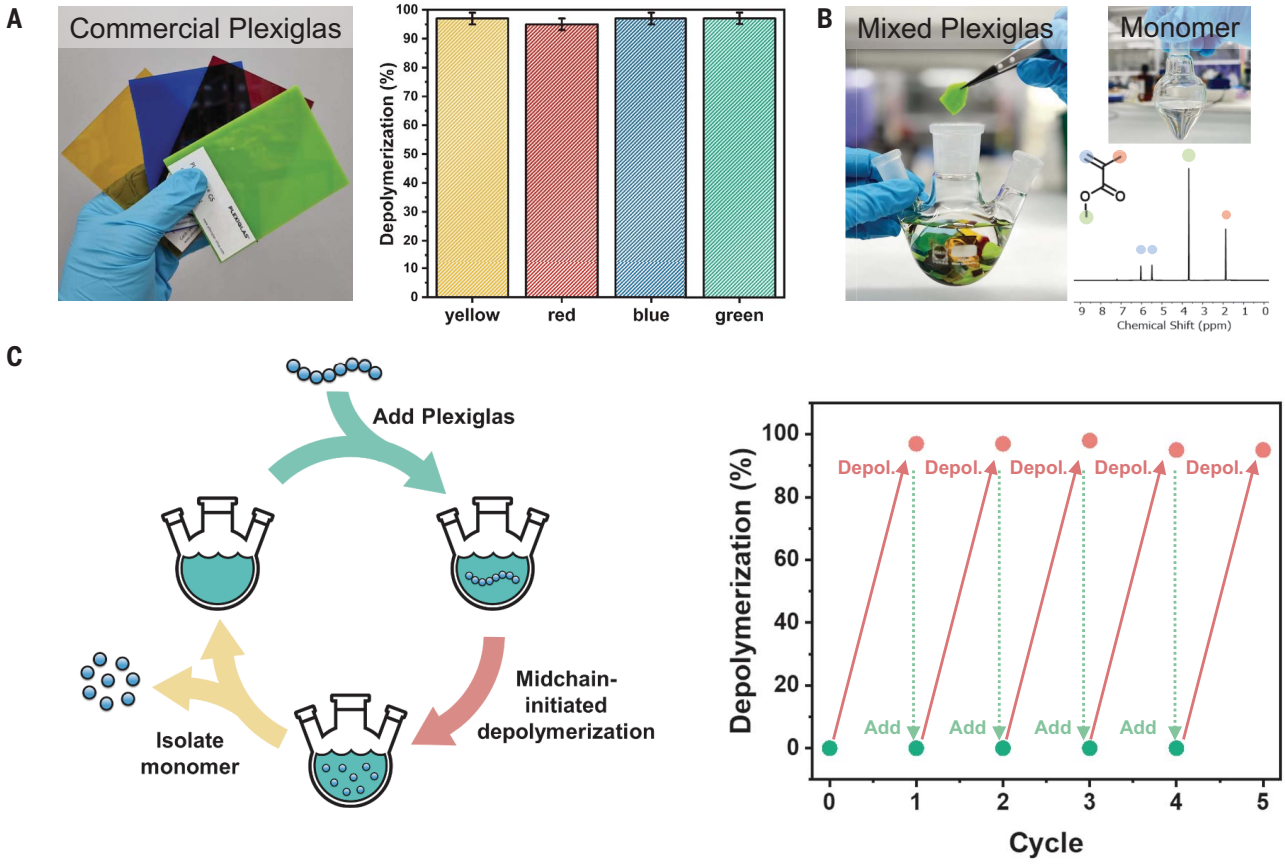

Fig. 4. Depolymerization of commercial Plexiglas. (**A**) Final depolymerization conversions of Plexiglas of varying color, (**B**) large-scale 2-M depolymerization of mixed Plexiglas, and (**C**) multicycle use of solvent for blue Plexiglas depolymerization. Error bars represent the standard deviation of >3 experiments. ppm, parts per million.

initiation. To this end, a series of polymers with various end groups were investigated. Different end groups were introduced by synthesizing PMMA through anionic polymerization (C–H end group), conventional free radical polymerization (mixture of C–H and C=C end groups), and ATRP (C–Cl end group) (table S3). In addition, PMMA terminated by a 2-cyano-2-propyl group (C–C end group) was synthesized by removing the end group of PMMA-DTB with excess radical initiator (azobisisobutyronitrile) (fig. S5). In accordance with our hypothesis, all samples underwent >95% depolymerization under 415-nm irradiation, further evidencing the end group–independent nature of this reaction (Fig. 2A). Even anionically synthesized PMMA underwent an efficient depolymerization (99%) despite it being the least reactive form of PMMA, reported to be thermally stable up to ~350°C (*30*). Under our conditions, depolymerization seemed to be occurring at significantly lower temperatures and in the absence of preinstalled weak bonds, opening up the possibility to potentially depolymerize commercial PMMA products.

To further investigate this unorthodox depolymerization pathway, PMMA synthesized by free radical polymerization (M_n = 331,600 g/mol, $Đ$ = 1.90) was selected as the model system. Detailed kinetic analysis showed a gradual reduction in molecular weight, further supporting a main chain–initiated pathway (Fig. 2B). Notably, high conversions could be achieved at temperatures as low as 90°C (fig. S6), albeit at reduced rates. Next, we tested the light-dependent nature of this reaction, as an ideal depolymerization should only proceed on demand. Multiple on-off cycles were performed in 1,2-dichlorobenzene to assess any unwanted thermal depolymerization. In four on-off cycles (15 min on, 15 min off), depolymerization only commenced during the "on" periods, proving that light is an essential trigger of the reaction (Fig. 2C). Even after an additional 1-hour-long "off" period, the final conversion was unaffected (>97%), highlighting the robust nature of the methodology. These results starkly contrast with previous (photo)thermal depolymerization of Cl-terminated polymethacrylates in which a sharp decline in the end-group fidelity (and thereby the extent of depolymerization) was observed after prolonged exposure to heat and/or light (*26*, *44*).

Chain end– versus main chain–initiated depolymerization

To contextualize our findings within the current landscape of depolymerization approaches and assess industrial feasibility, we compared our methodology with the labile chain end–initiated approach (*28*). PMMA-DTB was used as a benchmark, as it is arguably the most depolymerizable version of PMMA, capable of undergoing ~90% depolymerization, albeit at low molecular weights (~6000 g/mol) (*28*). We first examined the effect of molecular weight on the final depolymerization conversion for PMMA-DTB through a previously established chain end–initiated depolymerization protocol in 1,4-dioxane. A major decline in the final conversion from 87 to 9% was observed as the molecular weight increased from 6200 g/mol to 175,300 g/mol, in line with previous reports on the inverse relationship between molecular weight and conversion (Fig. 2D and table S4) (*31*, *43*). By contrast, our main chain–initiated depolymerization showed consistent conversions of 90 to 98% across a broad range of molecular weights up to 1,642,200 g/mol (Fig. 2D, fig. S7, and tables S5 and S6). This stark

improvement can be attributed to multiple initiation points within a single chain until full depolymerization is attained. This attribute is particularly appealing, as industrially produced PMMA typically exhibits molecular weights in the range of 10^4 to 10^6 g/mol.

Next, we were interested in probing the effect of the butyl acrylate (BA) comonomers within the chain, as commercially produced PMMA typically contains a small fraction (~1%) of acrylate comonomers to prevent depolymerization during thermal processing. As such, statistical P(MMA-*co*-BA)-DTB copolymers (BA = 0 to 1.1 mol %) were first synthesized by RAFT polymerization (table S7). The copolymers were then subjected to conventional thermal chain end–initiated depolymerization, and the final conversions were normalized to that of the homopolymer. Notably, the presence of BA had a remarkably negative impact on the final conversion: A relative conversion of 25% was observed when 1.1 mol % BA was present (Fig. 2E and fig. S8). Such high sensitivity to acrylate content is reasonable when considering that a polymethacrylate chain can only depropagate until reaching a single acrylate unit, after which termination will be favored, thereby kinetically trapping the remainder of the PMMA chain from further depolymerization (fig. S9). Instead, these molecular roadblocks can be bypassed by initiating depolymerization at multiple points within the chain. Indeed, when the same P(MMA-*co*-BA)-DTB samples underwent our main chain–initiated depolymerization, a remarkable relative conversion of 90% was reached even for the highest BA content (1.1 mol %), once more highlighting the importance of a multipoint initiation approach for materials that closely mimic commercial plastics (Fig. 2E).

Lastly, we examined the role of a polymer's thermal history on its susceptibility to depolymerization, as commercial products are typically thermally processed (e.g., at 190 to 220°C) and exposed to heat in their lifetime. When PMMA-DTB was heated for 30 min at 190°C under N_2 prior to chain end–initiated depolymerization, a conversion of only 5% was reached (compared to 82% for nonpreheated pristine samples) owing to end-group degradation, as confirmed by the loss of the UV response in SEC (Fig. 2F and fig. S10). This highlights another limitation of RDRP-synthesized polymers, as their susceptibility to depolymerization depends on the preservation of the weakest bond in the chain. This observation was also confirmed by the Matyjaszewski group's report of limited depolymerization of preheated ATRP-synthesized polymers (*44*). By contrast, when a main chain–initiated approach was used, no detectable change in the final conversion (95%) was observed for PMMA after the same thermal pretreatment (Fig. 2F), thereby demonstrating high tolerance to the thermal history of waste plastics, which removes a major limitation of approaches that rely on labile bonds.

Proposed mechanism of a main chain–initiated depolymerization

A series of experiments were conducted to gain a clearer picture of the mechanism. The first step was to identify the species responsible for initiating the depolymerization. Our earlier experiments showed that main chain scission can only occur in DCB; in dioxane, negligible, if any, shift in the molecular weight was observed throughout the reaction (fig S3, D and F). In addition, when the DCB experiment was conducted in the dark, no scission took place (fig S3E). Various other chlorinated and nonchlorinated solvents were also used under 415-nm irradiation, and whereas xylene, dimethylsulfoxide, dimethylformamide, and anisole solutions showed no appreciable scission under light irradiation, 1,2,4-trichlorobenzene solutions exhibited scission and depolymerization in a similar fashion to DCB, further suggesting that a chlorinated solvent is indeed necessary for main chain scission to occur (Fig. 3A and figs. S11 and S12). From these results, we suspected photodissociation of C–Cl bonds, leading to the formation of a reactive Cl radical and, presumably, an aryl radical. Density functional theory (DFT) simulations confirmed that homolytic cleavage of the C–Cl bond is energetically favorable in the first excited state (Fig. 3B). This is attributed to the elongation of the C–Cl bond in its excited state, which increases the electron density in the σ^*_{C-Cl} orbital, thereby breaking the bond (fig. S13 and tables S8 and S9). However, a question remained regarding the absorption of visible light by DCB, as the UV–visible light spectrum of DCB in acetonitrile showed no detectable absorption above 290 nm (fig. S14). However, when neat DCB was analyzed with air as the background, a small yet distinct absorption band spanning from UV to violet (λ = 300 to 390 nm) was observed, with a molar absorptivity at peak wavelength of $\varepsilon = 4.5 \times 10^{-3}$ L mol^{-1} cm^{-1}. This absorption feature remained evident even after various purification methods (figs. S15 and S16 and table S10), strongly indicating that the observed absorption is intrinsic to the DCB molecule and not an artifact. Time-dependent DFT identified this absorption as the S_0 to S_1 transition involving a forbidden electronic transition from the nonbonding orbital of Cl to the benzene π^* orbital, which explains the observed extremely low molar absorptivity. Thermal contributions to C–Cl cleavage seemed minor, as PMMA could undergo scission even when irradiated at room temperature in DCB (fig. S17). It is also worth mentioning that excitation at wavelengths above the absorbance wavelength has been comprehensively reported by Barner-Kowollik and co-workers (*45*, *46*), further supporting the plausibility of photodissociation under our reaction conditions.

Photodissociation of DCB was supported by electron paramagnetic resonance (EPR) using N-*tert*-butyl-α-phenylnitrone as a spin trap to detect unstable radicals (*47*). The spectrum of irradiated pure DCB consisted of three components (Fig. 3C) that exhibit hyperfine couplings with ^{1}H, ^{14}N, and ^{35,37}Cl nuclei. From spectral simulations, these components were identified as aryl (green: ^{14}N = 1.43 G, ^{1}H = 0.20 G) and, most likely, Cl (red: ^{14}N = 1.21 G, ^{1}H was unresolved, ^{35}Cl = 0.58 G, ^{37}Cl = 0.50 G; salmon: ^{14}N = 1.26 G, ^{1}H and ^{35,37}Cl couplings were unresolved) radical adducts (see supplementary materials for further discussion). In the presence of PMMA, the spectrum can be well simulated with a single component, with parameters consistent with an alkyl radical (^{14}N = 1.46 G, ^{1}H = 0.32 G) and particularly close to those of secondary radicals, which can be attributed to PMMA fragments. Signals resembling aryl radicals were also observed with a 2,4,6-tri-*tert*-butylnitrosobenzene spin trap (fig. S18). Detection of chlorinated biphenyl species after irradiation of DCB further evidenced the formation of aryl radicals through homolytic C–Cl scission (fig. S19). Notably, these chlorinated biphenyls are only present in trace concentrations and can still function as active reagents that can initiate further depolymerization until complete dechlorination. With this evidence, we propose that the Cl radical generates a C-centered PMMA backbone radical through hydrogen atom transfer (HAT) of a backbone methyl or methylene unit (*48*), followed by β scission of the backbone and depolymerization under thermodynamically favorable conditions (Fig. 3D and figs. S20 to S23). A HAT pathway through a Cl radical was further supported by the detection of HCl during irradiation (fig. S24). Moreover, a HAT pathway proceeding from the backbone was supported by small-molecule chlorination experiments (figs. S25 to S38), retarded depolymerization kinetics for backbone-deuterated PMMA (kinetic isotope effect $k_H/k_D \approx 5$; fig. S39), high depolymerization conversions of polymethacrylates possessing various side chains (fig. S40 and table S11), and the depolymerization of poly(α-methylstyrene) (fig. S41). Notably, the depolymerization of poly(α-methylstyrene) confirms that decarboxylation is not a prerequisite in the depropagation of PMMA and that depropagation likely proceeds through the alkene-terminated fragment. To confirm that the Cl radical, rather than the aryl species, is indeed responsible for the scission, a nonaromatic chlorine solvent (1,1,2,2-tetrachloroethane) was used and also resulted in main chain scission and comparable conversions to that in DCB (Fig. 3B, fig. S42, and table S12). This finding further suggested that the main reactive species is indeed the chlorine radical. Notably, the Br equivalent of DCB

(i.e., 1,2-dibromobenzene) did not lead to either scission or depolymerization (Fig. 3B and fig. S11), presumably because of the lower reactivity of Br radicals toward aliphatic 1° and 2°C (sp^3)–H (bond-dissociation energy of HBr BDE_{HBr} = 87 kcal/mol versus BDE_{HCl} = 103 kcal/mol). When a DCB/xylene mixture (90/10 vol/vol) was used, much lower conversions (<10%) were reached in the same timeframe. Considering that the weak C–H bond of the xylene methyl and the stable benzylic radical formed after HAT, we postulated that the Cl radical preferentially reacts with xylene rather than the polymer, therefore suppressing both scission and the subsequent depolymerization. Naturally, these results exclude direct photolysis of the backbone, in line with the lack of scission in nonchlorinated solvents (fig. S11). Further evidence of the proposed Cl-induced HAT was seen when lower wavelengths (365 and 395 nm) resulted in faster scission and depolymerization kinetics (fig. S43 to S45). Despite the rate differences, similarly high final depolymerization conversions were reached in all cases (i.e., 95%). Instead, no scission was observed at higher wavelengths (i.e., 460 nm), likely owing to insignificant photoexcitation.

Depolymerization of Plexiglas

In the previous sections, we demonstrated the depolymerization of various PMMA samples resembling industrially produced PMMA (i.e., with various end groups and different comonomer concentrations). However, we were also interested in exploring the applicability of our developed methodology directly to commercial products. Commercial PMMA, often known by the tradename Plexiglas, typically contains a variety of undisclosed comonomers and additives, such as radical inhibitors, plasticizers, and dyes, which may interfere with the reaction. To investigate this, we purchased a series of different commercial Plexiglas materials with varying color (yellow, blue, red, and green), and transparency (4 to 64% transmission) (Fig. 4A, fig. S46, and table S13). All four samples were subjected to our depolymerization conditions without any prior purification. Notably, all four samples underwent near-quantitative depolymerization (94 to 98%) (Fig. 4A), highlighting the robust nature of this approach to additives and the immediate applicability of this strategy to commercial products. Furthermore, multigram-scale (16 g) reactions of a mixture of these samples could be conducted at a concentration (2 M) above the solubility limit of the solvent (1,2,4-trichlorobenzene, at 170°C to reduce viscosity and improve yield), and high-purity monomer (99%) could be simply distilled from the solution owing to the large difference in the boiling points (100° versus 213°C) (Fig. 4B, fig. S47, and table S14). It is worth noting that, at 2 M, a final depolymerization conversion of 51% (41% yield) was attained as the system reached a thermodynamic equilibrium (equilibrium monomer concentration $[M]_{eq} \approx 1.3$ M at 170°C). Upon distillation of the regenerated MMA, depolymerization could be further driven to similar final conversions (fig S48). Subsequently, we tested the possibility of reusing the solvent for multiple reactions by conducting a series of depolymerization-monomer evaporation cycles in the same solvent. Even after five cycles, near-quantitative (<95%) depolymerization could be reached with only a minor decrease in rate, suggesting a minor impact of impurity accumulation and showing promise in both process simplification and the economics of this methodology (Fig. 4C). For further scale-up and a higher number of cycles, solvent management will be important to reduce chlorocarbon waste generated from this process (e.g., minimizing solvent deterioration by removing unknown plastic additives prior to depolymerization). Lastly, we tested our methodology in a mixed-waste stream containing either polyethylene terephthalate (PET), low-density polyethylene (LDPE), polypropylene (PP), polyurethane (PU), or polyvinyl chloride (PVC). Overall, our depolymerization methodology proved highly compatible with PET, LDPE, PP, and PU (>90%), whereas moderate conversions (69 to 85%) were observed in the presence of PVC (table S15).

Conclusions and outlook

We have developed a one-step, main chain–initiated depolymerization methodology that operates at temperatures far lower than that of traditional pyrolysis without relying on "designer polymers." The method is therefore directly applicable to commercial polymers while yielding near-quantitative monomer recovery. Furthermore, versatility was demonstrated by depolymerizing PMMAs with high molecular weights (e.g., $M_n = 10^6$ g/mol) and those containing acrylate comonomers. Lastly, as the method does not rely on labile end groups, no special care to preserve end group fidelity is needed (e.g., preventing exposure to heat and light).

REFERENCES AND NOTES

1. G. W. Coates, Y. D. Getzler, *Nat. Rev. Mater.* **5**, 501–516 (2020).
2. Z. O. G. Schyns, M. P. Shaver, *Macromol. Rapid Commun.* **42**, e2000415 (2021).
3. S. Oh, E. E. Stache, *J. Am. Chem. Soc.* **144**, 5745–5749 (2022).
4. C. Jehanno *et al*., *Nature* **603**, 803–814 (2022).
5. O. G. Mountanea, E. Skolia, C. G. Kokotos, *Green Chem.* **26**, 8528–8549 (2024).
6. S. Zhang, M. Li, Z. Zuo, Z. Niu, *Green Chem.* **25**, 6949–6970 (2023).
7. F. Eisenreich, *Angew. Chem. Int. Ed.* **62**, e202301303 (2023).
8. R. Cao, D. Xiao, M. Wang, Y. Gao, D. Ma, *Appl. Catal. B* **341**, 123357 (2024).
9. H. Cui, X. Chen, F. Lan, B. An, X. Zhang, *Trends Chem.* **6**, 392–405 (2024).
10. E. Skolia, O. G. Mountanea, C. G. Kokotos, *Trends Chem.* **5**, 116–120 (2023).
11. B. A. Abel, R. L. Snyder, G. W. Coates, *Science* **373**, 783–789 (2021).
12. T. M. McGuire, A. Buchard, C. Williams, *J. Am. Chem. Soc.* **145**, 19840–19848 (2023).
13. C. Shi *et al*., *Chem* **7**, 2896–2912 (2021).
14. C. B. Godiya *et al*., *J. Environ. Manage.* **231**, 1012–1020 (2019).
15. G. Moad, in *Macromolecular Engineering*, N. Hadjichristidis, Y. Gnanou, K. Matyjaszewski, M. Muthukumar, Eds. (Wiley-VCH, ed. 2, 2022), pp. 1–61.
16. P. Krys, K. Matyjaszewski, *Eur. Polym. J.* **89**, 482–523 (2017).
17. K. Parkatzidis, H. S. Wang, N. P. Truong, A. Anastasaki, *Chem* **6**, 1575–1588 (2020).
18. D. T. Gentekos, R. J. Sifri, B. P. Fors, *Nat. Rev. Mater.* **4**, 761–774 (2019).
19. C. Boyer *et al*., *Chem. Rev.* **109**, 5402–5436 (2009).
20. C. Barner-Kowollik, *Handbook of RAFT polymerization* (Wiley, 2008).
21. M. R. Martinez, K. Matyjaszewski, *CCS Chem.* **4**, 1–36 (2022).
22. M. R. Martinez, F. De Luca Bossa, M. Olszewski, K. Matyjaszewski, *Macromolecules* **55**, 78–87 (2021).
23. M. R. Martinez, S. Dadashi-Silab, F. Lorandi, Y. Zhao, K. Matyjaszewski, *Macromolecules* **54**, 5526–5538 (2021).
24. M. R. Martinez, D. Schild, F. De Luca Bossa, K. Matyjaszewski, *Macromolecules* **55**, 10590–10599 (2022).
25. F. De Luca Bossa, G. Yilmaz, K. Matyjaszewski, *ACS Macro Lett.* **12**, 1173–1178 (2023).
26. K. Parkatzidis, N. P. Truong, K. Matyjaszewski, A. Anastasaki, *J. Am. Chem. Soc.* **145**, 21146–21151 (2023).
27. H. S. Wang, K. Parkatzidis, T. Junkers, N. P. Truong, A. Anastasaki, *Chem* **10**, 388–401 (2023).
28. H. S. Wang, N. P. Truong, Z. Pei, M. L. Coote, A. Anastasaki, *J. Am. Chem. Soc.* **144**, 4678–4684 (2022).
29. V. Bellotti, H. S. Wang, N. P. Truong, R. Simonutti, A. Anastasaki, *Angew. Chem. Int. Ed.* **62**, e202313232 (2023).
30. R. Whitfield, G. R. Jones, N. P. Truong, L. E. Manring, A. Anastasaki, *Angew. Chem. Int. Ed.* **62**, e202309116 (2023).
31. J. B. Young *et al*., *Chem* **9**, 2669–2682 (2023).
32. J. B. Young, J. I. Bowman, C. B. Eades, A. J. Wong, B. S. Sumerlin, *ACS Macro Lett.* **11**, 1390–1395 (2022).
33. S. Huang, X. Su, Y. Wu, X.-G. Xiong, Y. Liu, *Chem. Sci.* **13**, 11352–11359 (2022).
34. M. J. Flanders, W. M. Gramlich, *Polym. Chem.* **9**, 2328–2335 (2018).
35. Y. Sano, T. Konishi, M. Sawamoto, M. Ouchi, *Eur. Polym. J.* **120**, 109181 (2019).
36. G. R. Jones *et al*., *J. Am. Chem. Soc.* **145**, 9898–9915 (2023).
37. V. Raus, E. Čadová, L. Starovoytova, M. Janata, *Macromolecules* **47**, 7311–7320 (2014).
38. R. W. Hughes *et al*., *J. Am. Chem. Soc.* **146**, 6217–6224 (2024).
39. J. B. Young *et al*., *Angew. Chem. Int. Ed.* **63**, e202408592 (2024).
40. M. T. Chin *et al*., *J. Am. Chem. Soc.* **146**, 5786–5792 (2024).
41. J. De Tommaso, J.-L. Dubois, *Polymers* **13**, 2724 (2021).
42. M. Sponchioni, S. Altinok, *Advances in Chemical Engineering*, **vol. 60**, D. Moscatelli, M. Pelucchi, Eds. (Academic Press, 2022), pp. 269–287.
43. H. S. Wang, N. P. Truong, G. R. Jones, A. Anastasaki, *ACS Macro Lett.* **11**, 1212–1216 (2022).
44. M. R. Martinez, F. De Luca Bossa, M. Olszewski, K. Matyjaszewski, *Macromolecules* **55**, 78–87 (2021).
45. S. L. Walden, J. A. Carroll, A.-N. Unterreiner, C. Barner-Kowollik, *Adv. Sci. (Weinh.)* **11**, e2306014 (2024).
46. D. E. Fast *et al*., *Macromolecules* **50**, 1815–1823 (2017).
47. G. R. Buettner, *Free Radic. Biol. Med.* **3**, 259–303 (1987).
48. P. Ulanski, E. Bothe, K. Hildenbrand, C. von Sonntag, *Chemistry* **6**, 3922–3934 (2000).

ACKNOWLEDGMENTS

Funding: A.A. gratefully acknowledges ETH Zurich for financial support. N.P.T. acknowledges the award of a DECRA Fellowship from the ARC (DE180100076). H.S.W. acknowledges the award of the Swiss Government Excellence Scholarship (ESKAS; no. 2020.0324). This project received funding from the European Research Council (ERC) under the European Union's Horizon 2020 Research and Innovation Programme (DEPO; grant agreement no.

949219). G.J. acknowledges funding from NCCR Catalysis, a National Centre of Competence in Research funded by the Swiss National Science Foundation. We thank T. Nauser and M.-N. Antonopoulou for fruitful discussions. **Author contributions:** H.S.W. and A.A. conceived the initial idea and managed the overall project. H.S.W. designed and performed the experiments with input from M.A. (EPR experiments) and H.K. (DFT simulations). H.S.W. and A.A. cowrote the manuscript with input from M.A., N.P.T., H.K., T.-L.C., and G.J. **Competing interests:** H.S.W. (ETH Zurich) and A.A. (ETH Zurich) have filed a patent related to the depolymerization methodology (EUROP/259). Other authors declare that they have no competing interests. **Data and materials availability:** All data are available in the main text or the supplementary materials.

SUPPLEMENTARY MATERIALS

science.org/doi/10.1126/science.adr1637
Materials and Methods
Figs. S1 to S48
Tables S1 to S15
Reference (*49*)

Submitted 18 June 2024; accepted 13 January 2025
10.1126/science.adr1637